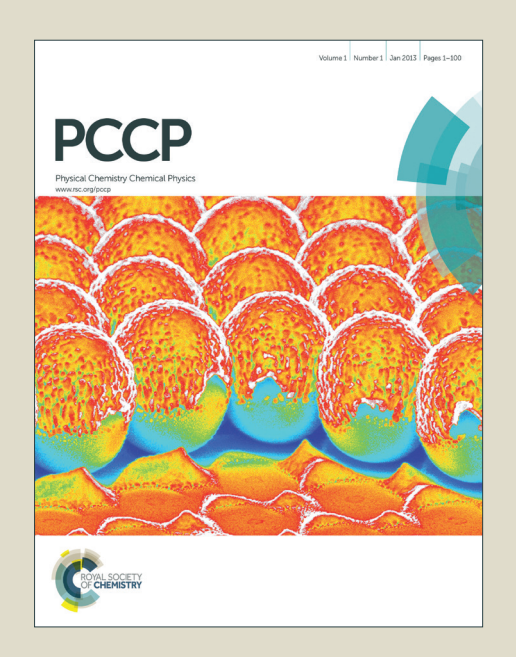


Accepted Manuscript



This is an *Accepted Manuscript*, which has been through the Royal Society of Chemistry peer review process and has been accepted for publication.

Accepted Manuscripts are published online shortly after acceptance, before technical editing, formatting and proof reading. Using this free service, authors can make their results available to the community, in citable form, before we publish the edited article. We will replace this Accepted Manuscript with the edited and formatted Advance Article as soon as it is available.

You can find more information about *Accepted Manuscripts* in the **Information for Authors**.

Please note that technical editing may introduce minor changes to the text and/or graphics, which may alter content. The journal's standard <u>Terms & Conditions</u> and the <u>Ethical guidelines</u> still apply. In no event shall the Royal Society of Chemistry be held responsible for any errors or omissions in this *Accepted Manuscript* or any consequences arising from the use of any information it contains.



Controlling the thermoelectric properties of polymers: application to PEDOT and Polypyrrole[†]

Mario Culebras, Belén Uriol, Clara Gómez, and Andrés Cantarero

Poly(3,4-ethylenedioxythiophene) (PEDOT) and polypyrrole (PPy) films have been prepared by an electrochemical method in a three electrode cell. The films have been obtained at different oxidation levels regarded as bipolaron, polaron and neutral states by varying the voltage, as it is usually done in conjugated heterocyclic polymers. The voltage (-0.2 < V < 1.0 V) has been applied *versus* a Ag/AgCl reference electrode, producing a variation of one order of magnitude in the electrical conductivity and the Seebeck coefficient of the films. In the voltage range explored, the electrical conductivity increases from 80 to 766 S/cm in PEDOT and from 15 to 160 S/cm in PPy, while the Seebeck coefficient decreases from 37.0 to 9.6 μ V/K for PEDOT and from 51.0 to 6.7 μ V/K for PPy. The thermal conductivity remains unchanged with the oxidation state of the film, $\kappa \approx 0.35 \pm 0.02$ W m $^{-1}$ K $^{-1}$ for PEDOT and 0.17 ± 0.02 W m $^{-1}$ K $^{-1}$ for PPy. A maximum thermoelectric efficiency of 1.4×10^{-2} for PEDOT and 6.8×10^{-3} for PPy have been achieved. These changes are related with the doping level of the polymer films and they can be accurately controlled by the applied voltage. In this work, we provide a very simple way to control and optimize the power factor or the figure of merit on conducting polymers.

1 Introduction

The lack of energy resources is a global problem. On one side, the oil reservoirs are limited, while on the other the energy demand is increasing along the years not only in developed countries, but also due to new demands which came into the market from countries like China and India with a growing rate of 5-8%. Water will also become a problem in the future, thus probably hydraulic plants will provide energy in a limited time difficult to evaluate. With this panorama in mind, new energy resources must be in operation soon at least to compensate the growth of the energy market. The most plausible alternative at the moment are the Nuclear Plants; being pragmatic they must be used at least during a few decades until enough energy can be supplied by photovoltaics, mill farms, biomass, and other clean/green energy production compatible with the sustainability of our planet. In the last years, thermoelectricity has arisen as a promising alternative to transform waste heat into electricity, via the Seebeck effect, or to complement photovoltaic cells, to keep them working in the maximum efficiency ¹. Unfortunately, the efficiency of thermoelectric devices has not been improved much in the last decades. But a few years from now, the scientific community started to work hard on thermoelectricity and we can expect a substantial growth of the efficiency in the next few years. How good is a thermoelectric material can be quantitatively written in terms of

Materials Science Institute, University of Valencia, PO Box 22085, 46071 Valencia, Spain. Fax: +34 963543633; Tel: +34 963544713; E-mail: andres.cantarero@uv.es † Electronic Supplementary Information (ESI) available: [details of any supplementary information available should be included here]. See DOI: 10.1039/b000000x/

the dimensionless figure of merit ZT, which is defined as:

$$ZT = \frac{S^2 \sigma}{\kappa} T \quad , \tag{1}$$

where S is the Seebeck coefficient, σ the isothermal electrical conductivity, κ the thermal conductivity and T the absolute temperature. Since the Seebeck coefficient goes to the square, it seems more important to increase S, even if σ decreases in a reasonable amount. Actually, many times, when we work with similar materials, it is enough to use the power factor $PF \equiv S^2 \sigma$ to know if the thermoelectric efficiency is being improved.

Nowadays, the best thermoelectric materials in terms of ZT are semiconductors. For instance, $\mathrm{Bi}_2\mathrm{Sb}_3$ is a good thermoelectric material used in low temperature applications 2 , while $\mathrm{Bi}_2\mathrm{Te}_3$ and PbTe can be used for room temperature applications $^{3-7}$ and $\mathrm{Si}_{1-x}\mathrm{Ge}_x$ alloys 8 and half-Heusler compounds 9 in high temperature applications, and skutterudites in medium-temperature thermoelectric modules 10 . The figure of merit was around one during many years, until the beginning of the 90's of last century. After the seminal work of Hicks and Dresselhaus 11 it was clear that, reducing the dimensionality (for instance by building a superlattice) of the semiconductor, the figure of merit would increase, peaking the Fermi level in a maximum of the density of electronic states. Unfortunately, in more than 20 years of research, ZT has increased only in a factor of 3.

In the last 10-15 years, organic materials have become important in optoelectronics 12,13 , both in solar cells and light emitting diodes, and more recently in thermoelectricity 14,15 , especially in thin films, where the polymer chains remains basically in two di-

mensions 16,17 . Several intrinsically conducting polymers (ICPs) have been successfully used, increasing the figure of merit several orders of magnitude 15,18 , until values very close to that of inorganic materials. Polymers present, in addition, many advantages over inorganic materials: non scarcity of raw materials, lack of toxicity, lower cost of production and many others. Thinking of inorganic compounds, one of the barriers which does not allow the improvement of ZT is its high thermal conductivity, which is mainly produced by the heat transported by phonons. Polymers have a thermal conductivity at least one order of magnitude smaller than any semiconductor. In the next years, we need to work on the improvement of the Seebeck coefficient and the electrical conductivity on ICPs.

The efficiency of thermoelectric polymers is largely dependent on the doping level of the material since it modifies both S and σ . These parameters are actually not completely independent. Thus, by increasing the doping level the electrical conductivity increases but the Seebeck coefficient decreases making it necessary to find a balance between them in order to obtain the optimum value of ZT, which actually is given by the power factor PF^{19-23} . One of the methods more commonly used to control the doping level of polymers is the chemical de-doping ^{19–21}. This method changes the doping level by using reducting agents such as hydrazine or tetrakis(dimethylamino)ethylene (TDAE) 19-21. Another procedure to control the doping level is the electrochemical doping/dedoping ^{22,23}, that offers certain advantages. The first one is that the oxidation state (doping level) can be easily controlled by using an electrochemical cell. A second advantage is the absence of a purification steps, required in other methods, which again simplifies the process. Finally, what moreover it is a novelty, produces a free standing film, meaning that it does not need the electrode in order to work.

In this work, we have synthesized free-standing films by electrochemical deposition of two conducting polymers, poly(3,4-ethylenedioxythiophene) (PEDOT) and polypyrrole (PPy). The electrochemical cell has been employed to change the doping level of the polymers in order to control the thermoelectric properties. We describe a new methodology able to control the thermoelectric properties of conducting polymers, such as PEDOT and PPy, able to supply the required properties for a given application. This is of great importance in future applications as for instance the use of polymer matrices in thermoelectric nanocomposites or as sensitive element in temperature sensors.

2 Experimental

2.1 Materials

The reactants used in this work are pyrrole, 3,4-ethylenedioxythiophene (EDOT), lithium perchlorate (LiClO₄), ethanol and acetonitrile, were purchased from Sigma Aldrich.

2.2 Synthesis of PEDOT

The electrochemical synthesis of PEDOT was carried out at room temperature in a three electrode cell following the procedure described in a previous work ¹⁹. The working electrode was a gold coated PET surface for SEM and transport measurements, while

an ITO coated glass was used for cyclic voltammetry and absorbance measurements. A platinum grid acted as the counterelectrode and the Ag/AgCl electrode acted as the reference one. PEDOT was polymerized from a 0.01 M solution of EDOT and LiClO₄ 0.1 M in acetonitrile. The electrochemical polymerization was made at a deposition intensity of 3 mA during 1.5 min over the working electrode surface. Films of 120-130 nm thickness were obtained. The gold layer of the corresponding working electrode was removed with an acid solution (HNO₃:HCl ratio 1:3) after the film deposition. Finally, the deposited PEDOT films were rinsed several times with water and ethanol to remove the untreated monomer and then dried in air at room temperature.

2.3 Synthesis of Polypyrrole

Polypyrrole films were also prepared at room temperature by the electrochemical polymerization method in a conventional three electrode system. The working electrode was a stainless steel electrode for SEM and transport measurements while an ITO electrode was used for voltamperometry and absorbance measurements. A platinum grid acted as the counter-electrode and the Ag/AgCl electrode was used as reference. Polypyrrole was polymerized from a 0.01 M solution of pyrrole and LiClO₄ 0.1 M in acetonitrile. The electrochemical polymerization was made at a deposition intensity of 3 mA. The films, grown on the ITO electrode during 1.5 min, were 120-130 nm thick, whereas those obtained on stainless steel electrodes during 4 h were 100 μ m. Finally, the deposited PPy films were rinsed several times with water and ethanol to remove the untreated monomer and then dried in air at room temperature. The layer of PPy was detached from the steel surface and transferred into a glass substrate for measurements purposes.

2.4 Electrochemical reduction of polymers

The electrochemical reduction of the polymeric samples was carried out in an Ivium-n-Stat: multi-channel electrochemical work-station under computer control. The three electrodes cell was formed by the ITO coated by the polymer (PEDOT or PPy) as the working electrode, the platinum grid as the counter-electrode, and the Ag/AgCl electrode as the reference one in a 0.1 M of LiClO $_{\!4}$ in acetonitrile solution. The polymer samples were subjected to several voltages vs the Ag/AgCl reference electrode, in order to determine the absorbance and the transport properties (electrical conductivity and Seebeck coefficient) at different reduction states.

2.5 Characterization

The thickness of the polymer films was determined with a Dektak profilometer. The morphology of the polymers was determined by scanning electron microscopy with a Hitachi 4800 S microscope at an acceleration voltage of 20 kV and at a working distance of 14 mm for gold-coated surfaces. Cyclic voltammetry was performed with an Ivium-n-Stat: multi-channel electrochemical workstation under computer control. The three electrode cell was the same as that for polymerization. The films were equilibrated at -2.0 V and -3.0 V for 2 min for PEDOT and PPy, respectively, before

cyclic at 20 mV/s voltammetric measurements. The absorbance measurements were performed in a Shimadzu UV-2501PC UV-Vis spectrophotometer from 1100 to 300 nm. The thermal conductivity was determined with the aid of modulated differential scanning calorimetry (MDSC) according to the ASTM E1952-11 standard test method. This method is valid to measure thermal conductivities of polymeric materials with values within the range 0.1-1 W m $^{-1}$ K $^{-1}$. The MDSC measurements were performed in a DSC Q-20 TA Instruments calibrated with indium and sapphire. All MDSC measurements were carried out at 300 K in modulated conditions with a period of 80 s and ± 1 K of temperature amplitude.

The electrical conductivity was determined by the Van der Paw method ²⁴. A Keithley 2400 multimeter was used as driving source and voltmeter. The conductivity of the sample is obtained by solving the Van der Pauw equation:

$$e^{-\pi dR_1\sigma} + e^{-\pi dR_2\sigma} = 1$$
 , (2)

where d is the sample thickness, R_1 and R_2 are the resistances between two different contacts, and σ the electrical conductivity. The Seebeck coefficient has been determined with a home-made apparatus composed by a Lakeshore 340 temperature controller and a Keithley 2750 Multimeter/Switching System. The Seebeck coefficient is obtained as the ratio between the electrical potential, ΔV , and the temperature difference, ΔT , that is:

$$S = \frac{\Delta V}{\Delta T} \quad . \tag{3}$$

3 Results and discussion

Scanning electron microscope (SEM) images of the PEDOT and PPy films obtained after the electrochemical polymerization are depicted in Figure 1. The surface morphology of PEDOT (Figure 1a) shows a homogeneous and compact surface with a certain degree of roughness of nearly interconnected polymer chains and voids in between ^{19,25}. The SEM surface image of PPy (Figure 1b) shows typical granular (cauliflower) morphologies distributed over the substrate surface and densely packed ^{26,27}. The differences between the morphology found in the SEM images can be attributed to the different interaction between the polymers and the solvent, in our case acetonitrile ²⁸.

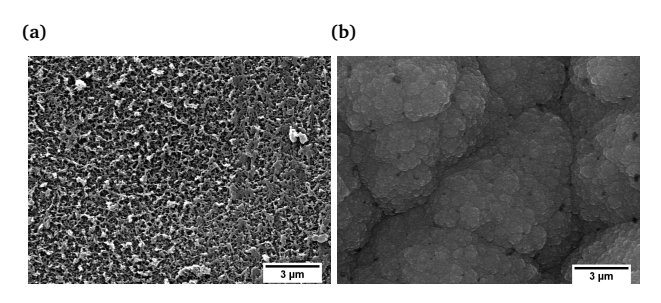


Fig. 1 SEM images of: a) PEDOT and b) PPy films surfaces after electrochemical polymerization.

Cyclic voltammetry between -3 and +1.5 V at a rate of 20 mV/s was performed on the PEDOT and PPy films (Figure 2) in order

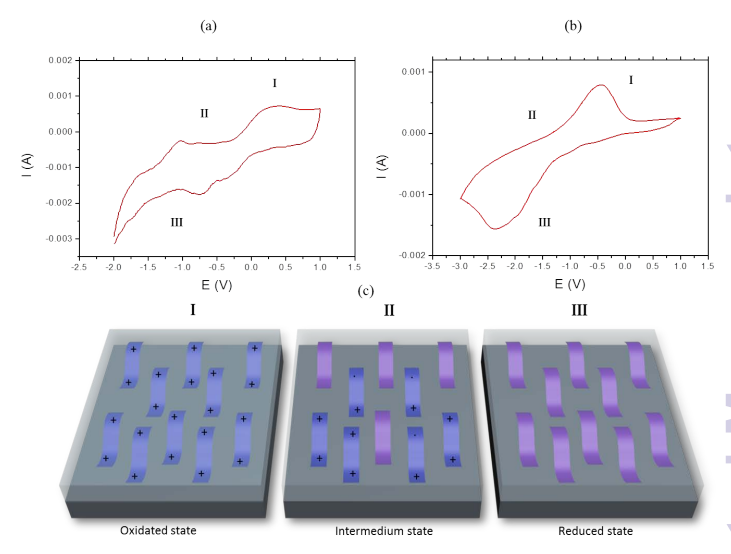
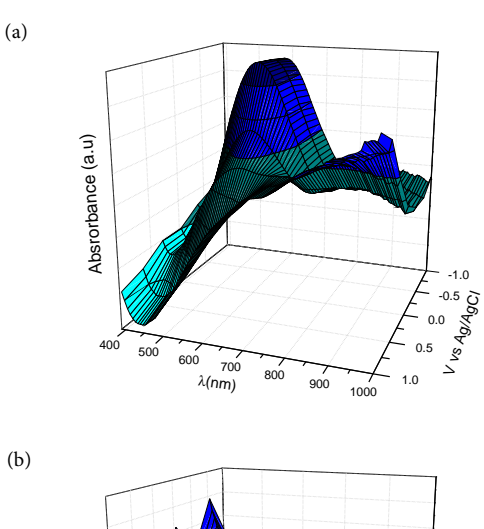


Fig. 2 Cyclic voltammetry of: a) PEDOT and b) PPy. c) Scheme of polymer electronic states as a function of the oxidation/reduction level.

to determine the voltage where the oxidation/reduction polymer species appear. The shape of the voltammogram with anodic (I) and catodic (III) peaks related with the oxidation and reduction processes is similar to those reported in the literature $^{29-36}$. The peak appearing at positive current values is related to the oxidation of the polymer, while that shown at negative currents is related to the reduction states (Figure 2). The reduction or cathodic peak appears in the range from -1.0 to +0.2 V while the oxidation peak is located in a potential range between 0 and 0.5 V (see Fig 2a) for PEDOT. Polypyrrole films depict a clear oxidation peak in the range from -1.0 to 0 V and a reduction peak in the range from -2.5 to -1.5 V (see Figure 2b). Figure 2c shows a scheme on the evolution of the polymer chains depending on the applied voltage. At oxidation potentials, the polymer chains are in a bipolaronic state, at intermediate potentials there is a mixture between bipolaronic, polaronic and neutral states and finally at reduction potentials the chains are in their neutral states.

The nature of the doping states of conjugated polymers is still a matter of debate. A high doping level is desirable to improve the applications of conducting polymers; in the present case thermoelectric devices. Cyclic voltammetry has been performed to know the voltage values where the oxidized and reduced species appear. These voltages will change the doping state of the polymer and, as expected, the thermoelectric efficiency. In order to change the doping level of PEDOT and PPy, different voltages (*V vs* Ag/AgCl, taken as reference voltage) have been applied to the films, until the current remained unchanged. In this way, we have different doped polymers from neutral to bipolaron. Optical absorption, electrical and thermal conductivity, and Seebeck coefficient have been determined in those doped films.

Ultraviolet-visible (UV-Vis) spectrochemical curves are shown in Figure 3 for PEDOT and PPy films deposited on an indium tin oxide (ITO) coated glass. The spectra depict different bands related with different oxidation states due to the electrochemical doping. A broad absorption band centered at 900 nm related



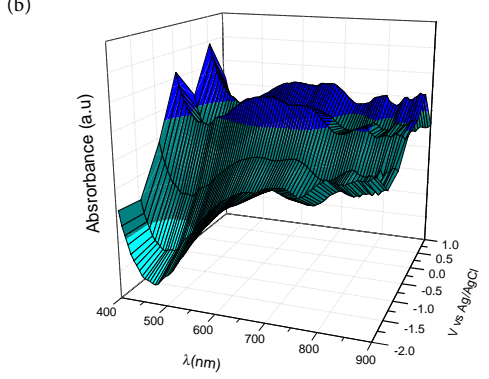


Fig. 3 UV-Vis spectra of: a) PEDOT and b) polypyrrole as a function of different applied voltages *vs* Ag/AgCl on ITO coated glass electrodeposited polymer films.

with the oxidized PEDOT state (0.0 < V < 1.0 V) appears during the doping process and it is related to polaron and bipolaron states³⁶. However, an absorption band centered at 600 nm appears in the PEDOT reduced state (V = -1.0 V), that decreases its intensity as the applied voltage increases, that is, as the polymer changes from a reduced to an oxidized state, related to the $\pi - \pi^*$ transition ^{33–38}. Thus, changing the doping states of the PEDOT chains from bipolarons/polarons to neutral states results in changes in the optical properties of the polymer. The colour of the polymer changes from dark blue in the reduced state to light blue in the oxidized (bipolaron) state. Figure 3b shows the UV-Vis spectrum of PPy films obtained at different doping levels. The absorption band between 500-900 nm at high applied voltages is related with the polaronic and bipolaronic (oxidized) states of PPy³⁵. The band at 300-500 nm, related to the absorption of the neutral or reduced state of PPy35, cannot be observed since it overlaps with the substrate signal (PET-ITO). The colour of PPv changes from a neutral yellow form to blue-green for the fully oxidized, bipolaron state.

Figure 4 shows the electrical conductivity, Seebeck coefficient and the power factor of PEDOT (Figure 4a) and PPy (Figure 4b) films as a function of the applied voltage (vs Ag/AgCl). In both cases, the electrical conductivity increases with the applied voltage or the oxidation state of the polymers. As the applied voltage changes from negative to positive, the polymers change from

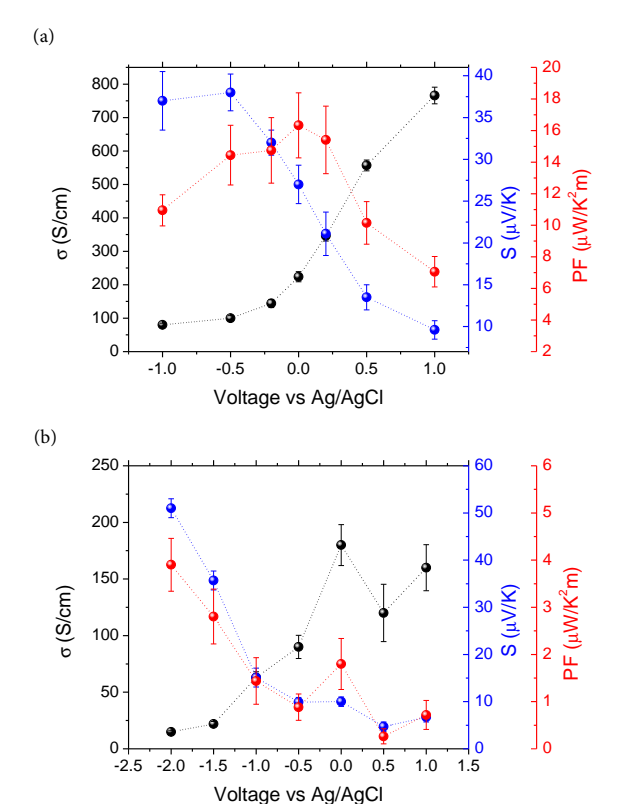


Fig. 4 Electrical conductivity, Seebeck coefficient and power factor of a) PEDOT and b) PPy as a function of voltage referred to the Ag/AgCl electrode.

reduced to neutral and to an oxidized state, i. e. a bipolaron state as corroborated by cyclic voltammetry and UV-Vis measurements. The electrical conductivity of PEDOT changes from 80 S/cm at -1.0 V to 766 S/cm at +1.0 V. These values are of the same order of magnitude than those found in the literature. For example PEDOT:PSS (PEDOT:poly(styrenesulfonate)) doped with dimethyl sulfoxide (DMSO) has an electrical conductivity between 500 and 1000 S/cm^{20,25,39,40}. The electrical conductivity of PPy increases from 15 S/cm at -2.0 V to 160 S/cm at +1.0V. At the highest oxidation level, we obtain similar values to that reported for PPy:PF $_6$ (100 – 600 S/cm) 41 , but higher than those obtained for PPy composites such as PPy/MWCNTs, 70 S/cm⁴², or PPy/graphene nanosheets, 40 S/cm⁴³. The opposite trend has been observed in the variation of the Seebeck coefficient (Figure 4). The Seebeck coefficient of PEDOT decreases from 37.0 μ V/K at -1.0 V to 9.6 μ V/K at +1.0 V whereas the Seebeck coefficient of PPy changes from 51.0 μ V/K at -2.0 V to 6.7 μ V/K at +1.0 V (always referred to the Ag/AgCl reference electrode). The values of S obtained for the PEDOT films are similar to those reported in Ref. ¹⁹. However, the values of the Seebeck coefficient obtained in this work for PPy are the highest values ever measured ¹⁸.

The *PF* corresponding to PEDOT and PPy has also been plotted in Figure 4. The maximum *PF* is 16.3 μ V K⁻¹m⁻² for PEDOT at 0.01 V, while for the case of PPy the maximum value has been reached at -2.0 V, 3.9 μ V K⁻¹m⁻². These values are related to an intermediate polaron structure for PEDOT and a reduced, neutral state for PPy due to the relationship between the Seebeck coeffi-

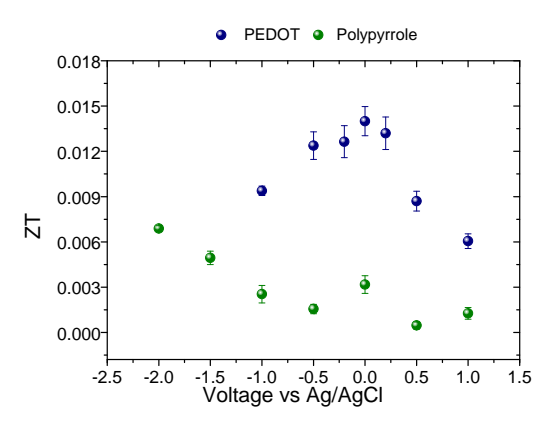


Fig. 5 ZT of PEDOT and PPy as a function of applied potential at 300 K.

cient and the electrical conductivity.

In order to supply values of ZT, the thermal conductivity has been determined for the different samples, being independent of the doping level of the samples. The values obtained at 300 K were $0.35 \pm 0.02 \text{ W m}^{-1}\text{K}^{-1}$ for PEDOT and $0.17 \pm 0.02 \text{ W m}^{-1}\text{K}^{-1}$ for PPy. We have checked that the thermal conductivity does not change with the applied voltage. Two recent papers reported a small anisotropy in the thermal conductivity of PEDOT^{44,45} and a certain dependence with the electrical conductivity. The in-plane thermal conductivity increases with increasing σ , while the perpendicular thermal conductivity remains constant. This can be interpreted from the configuration of the polymeric chains (the amount of chains in-plane as compare to off-plane). In a very thin film, as it is the case here, the chains remain in plane and the thermal conductivity actually corresponds to the in plane conductivity, even if we produce a pellet crashing the film. The values measured in the present work using a DSC are in agreement with previous literature results ^{19,21,46}.

The efficiency of a thermoelectric device, ZT, calculated from equation (1) has been plotted in Figure 5 for the different samples. The highest value of ZT were 6.8×10^{-3} for PPy and 1.4×10^{-2} for PEDOT, using the values of thermal conductivity obtained form our DSC measurements. These results are of the same order of magnitude as other recently reported on conducting polymers 15,18 .

4 Conclusions

Concluding, Free-standing films of PEDOT and PPy with high electrical conductivity have been prepared by electrochemical polymerization in a three electrode cell using a Ag/AgCl reference electrode. The electrical conductivity and Seebeck coefficient of the polymer films can be controlled by applying different potential differences to the films. The electrical conductivity is maximum at oxidation potentials of $0.5-1.0~\rm V$ for PEDOT and $0.0-1.0~\rm V$ for PPy, while the Seebeck coefficient is maximum at reduction potentials of $-1.0~\rm V$ for PEDOT and $-2.0~\rm V$ for PPy. The maximum thermoelectric efficiency has been obtained at $0.01~\rm V$ for PEDOT and at $-2.0~\rm V$ for PPy. The results show a very simple way to control and optimize ZT in conducting polymers.

References

- R. Ahiska and H. Mamur, Int. J. Renew. Energy Res., 2014, 4, 128–136.
- 2 D.-H. Lee, J.-U. Lee, S.-J. Jung, S.-H. Baek, J.-H. Kim, D.-I. Kim, D.-B. Hyun and J.-S. Kim, J. Electron. Mater., 2014, 43, 2255–2261.
- 3 Y. Gelbstein and J. Davidow, Phys. Chem. Chem. Phys., 2014, 16, 20120–20126.
- 4 T. C. Hasapis, S. N. Girard, E. Hatzikraniotis, K. M. Paraskevopoulos and M. G. Kanatzidis, *J. Nano Res.*, 2012, 17, 165–174.
- 5 P. H. Le, C.-N. Liao, C. W. Luo and J. Leu, J. Alloy. Compd., 2014, 615, 546–552.
- 6 B. Poudel, Q. Hao, Y. Ma, Y. Lan, A. Minnich, B. Yu, X. Yan, D. Wang, A. Muto, D. Vashaee, X. Chen, J. Liu, M. S. Dresselhaus, G. Chen and Z. Ren, *Science*, 2008, 320, 634–638.
- 7 R. Venkatasubramanian, E. Siivola, T. Colpitts and B. O'Quinn, *Nature*, 2001, **413**, 597–602.
- 8 N. Stein, N. Petermann, R. Theissmann, G. Schierning, R. Schmechel and H. Wiggers, *J. Mater. Res.*, 2011, **26**, 1872–1878.
- 9 E. Rausch, B. Balke, S. Ouardi and C. Felser, *Phys. Chem. Chem. Phys.*, 2014, **16**, 25258–25262.
- 10 J. R. Salvador, J. Y. Cho, Z. Ye, J. E. Moczygemba, A. J. Thompson, J. W. Sharp, J. D. Koenig, R. Maloney, T. Thompson, J. Sakamoto, H. Wang and A. A. Wereszczak, *Phys. Chem. Chem. Phys.*, 2014, 16, 12510–12520.
- 11 L. D. Hicks and M. S. Dresselhaus, *Phys. Rev. B*, 1993, **47**, 12727–12731.
- 12 Z. Guo, D. Lee, Y. Liu, F. Sun, A. Sliwinski, H. Gao, P. C. Burns, L. Huang and T. Luo, *Phys. Chem. Chem. Phys.*, 2014, 16, 7764–7771.
- R. C. Chiechi and J. C. Hummelen, ACS Macro Letters, 2012,
 1, 1180–1183.
- 14 S. K. Yee, N. E. Coates, A. Majumdar, J. J. Urban and R. A. Segalman, *Phys. Chem. Chem. Phys.*, 2013, **15**, 4024–4032.
- M. Culebras, C. M. Gomez and A. Cantarero, *Materials*, 2014,
 7, 6701–6732.
- 16 Q. Wei, M. Mukaida, K. Kirihara and T. Ishida, *ACS Macro Lett.*, 2014, **3**, 948–952.
- 17 D. Wang, W. Shi, J. Chen, J. Xi and Z. Shuai, *Phys. Chem. Chem. Phys.*, 2012, **14**, 16505–16520.
- 18 Y. Du, S. Z. Shen, K. Cai and P. S. Casey, *Prog. Polym. Sci.*, 2012, **37**, 820–841.
- 19 M. Culebras, A. Cantarero and C. M. Gómez, *J. Mater. Chem. A*, 2014, **2**, 10109–10115.
- 20 S. H. Lee, H. Park, S. Kim, W. Son, I. W. Cheong and J. H. Kim, *J. Mater. Chem. A*, 2014, **2**, 7288–7294.
- 21 O. Bubnova, Z. U. Khan, A. Malti, S. Braun, M. Fahlman, M. Berggren and X. Crispin, *Nat Mater*, 2011, **10**, 429–433.
- 22 T. Park, C. Park, B. Kim, H. Shin and E. Kim, *Energy Environ. Sci.*, 2013, **6**, 788–792.
- 23 O. Bubnova, M. Berggren and X. Crispin, J. Am. Chem. Soc.,

- 2012, 134, 16456-16459.
- 24 L. J. Van Der Pauw, Philips Techinical Review, 1958, 20, 220–224
- 25 J. Feng-Xing, X. Jing-Kun, L. Bao-Yang, X. Yu, H. Rong-Jin and L. Lai-Feng, *Chin. Phys. Lett.*, 2008, **25**, 2202–2205.
- 26 D. Ge, J. Mu, S. Huang, P. Liang, O. U. Gcilitshana, S. Ji, V. Linkov and W. Shi, *Synth. Met.*, 2011, **161**, 166–172.
- 27 J. V. Thombare, M. C. Rath, S. H. Han and V. J. Fulari, *Journal of Semiconductors*, 2013, **34**, 103002.
- 29 Randriamahazaka, H., J. Phys. Chem. C, 2007, 111, 4553–4560.
- 30 A. Aydin and I. Kaya, Org. Electron., 2013, 14, 730-743.
- 31 P. Anjaneyulu, V. Varade, C. S. S. Sangeeth, K. P. Ramesh and R. Menon, *J. Phys. D-Appl. Phys.*, 2014, **47**, 505106.
- 32 A. Diaz, K. Kanazawa and G. Gardini, *J. Chem. Soc.-Chem. Commun.*, 1979, 635–636.
- 33 S. Garreau, G. Louarn, J. Buisson, G. Froyer and S. Lefrant, *Macromolecules*, 1999, **32**, 6807–6812.
- 34 H. Ahonen, J. Lukkari and J. Kankare, *Macromolecules*, 2000, 33, 6787–6793.
- 35 P. Rapta, A. Neudeck, A. Petr and L. Dunsch, *J. Chem. Soc.-Faraday Trans.*, 1998, **94**, 3625–3630.
- 36 S. Garreau, J. Duvail and G. Louarn, Synth. Met, 2001, 125, 325–329.
- 37 X. Chen and O. Inganas, J. Phys. Chem., 1996, **100**, 15202–15206.
- 38 J. Wang, K. Cai and S. Shen, *Org. Electron.*, 2015, **17**, 151 158.
- 39 G.-H. Kim, L. Shao, K. Zhang and K. P. Pipe, *Nat. Mater.*, 2013, **12**, 719–723.
- 40 K.-C. Chang, M.-S. Jeng, C.-C. Yang, Y.-W. Chou, S.-K. Wu, M. A. Thomas and Y.-C. Peng, J. Electron. Mater., 2009, 38, 1182–1188.
- 41 K. Sato, M. Yamaura, T. Hagiwara, K. Murata and M. Tokumoto, *Synth. Met.*, 1991, **40**, 35–48.
- 42 J. Wang, K. Cai, S. Shen and J. Yin, *Synth. Met.*, 2014, **195**, 132–136.
- 43 S. Han, W. Zhai, G. Chen and X. Wang, *RSC Adv.*, 2014, 4, 29281–29285.
- 44 A. Weathers, Z. U. Khan, R. Brooke, D. Evans, M. T. Pettes, J. W. Andreasen, X. Crispin and L. Shi, *Advanced Materials*, 2015, **27**, 2101–2106.
- 45 J. Liu, X. Wang, D. Li, N. E. Coates, R. A. Segalman and D. G. Cahill, *Macromolecules*, 2015, **48**, 585–591.
- 46 J. Wu, Y. Sun, W. B. Pei, L. Muang, W. Xu and Q. Zhang, *Synth. Met.*, 2014, **196**, 173–177.

6 |